JOURNAL OF MATERIALS SCIENCE 22 (1987) 1682–1686

Influence of dissolution rate on crack growth and fatigue of Na_2O–Al_2O_3–B_2O_3–SiO_2 glasses

ECKHARD GEHRKE, M. HÄHNERT, CH. ULLNER
Zentralinstitut für anorganische Chemie der Akademie der Wissenschaften der DDR, Rudower Chaussee 5, 1199 Berlin, German Democratic Republic

Fracture toughness, macroscopic crack growth and dynamic fatigue of glasses of the system $15Na_2O-4Al_2O_3-xB_2O_3-(81-x)SiO_2$ are studied. The fracture toughness as a function of B_2O_3 content correlates to the dependence of elastic modulus which has a maximum between 20 and 30 mol%. The shape of the crack growth curve changes characteristically. Region 1 of the curves normalized to K_{Ic} is shifted to higher crack growth velocities (smaller K_I/K_{Ic} values, respectively) for increasing B_2O_3 content. The rise of velocity correlates approximately to the dissolution rate of the glasses in water. The determination of the slope in region 1 is problematic, particularly for poorly resistant glasses. The slope n of the crack growth velocity fitted by the power law decreases above 20 mol% B_2O_3 in correspondence with the results of the dynamic fatigue ($23 > n > 7$). A clear fatigue limit at one fifth of the inert strength occurs in glasses with B_2O_3 content above 20 mol%.

1. Introduction

Investigations of the effect of the glass composition [1] and the ambient medium (partial vapour pressure [2], pH value [3, 4]) on the position and the slope of region 1 of the characteristic multiregional crack growth curve have shown that the crack growth in this region is determined by the rate of reaction between glass at the crack tip and water. The elementary mechanism of this reaction is explained by stress enhanced network dissolution [1] or stress assisted chemical bond rupture [5].

In the present paper the influence of the network formers on the parameters of crack growth and fatigue is investigated for the example of sodiumalumoborosilicate glasses. Particularly the correlation to the corrosion behaviour of the glasses is studied.

2. Experimental procedures

Glasses of the composition $15Na_2O-4Al_2O_3-xB_2O_3-(81-x)SiO_2$ were melted in Pt–Rh crucibles and cast to ingots (crack growth measurements) or drawn to rods (fatigue experiments). All samples were annealed from 50 K above the transformation temperature to room temperature at 5 K min^{-1}.

Amounts of Al_2O_3 were added to reduce the tendency to phase separation which is known for glasses of this system. The measurements of crack growth were performed by the double-cantilever beam method on samples having the dimensions 75 × 24 × 2 mm^3. The crack growth rate below 10^{-3} msec^{-1} was measured by means of a measuring microscope. Above 10^{-4} msec^{-1} the crack growth rate was determined through the modulation of the fracture surface by sound waves in burst mode [6].

The investigation of the strength was carried out by means of electronically controlled test equipment poor in inertia, furnished with electromagnetic power generation [7]. The specimens were rods (diameter 5 mm) abraded by emery paper (600 grit) and loaded in a three-point bending (span length 50 mm) at room temperature in water or at liquid nitrogen temperature (inert strength σ_s). The Young's modulus was determined by run time measurement. The dissolution rate in water was calculated from the flame photometric measurement of the leached Na_2O in the solution as a function of corrosion time.

At higher B_2O_3 contents the dissolution rate can be determined additionally by direct measurement of the decreased diameter of the rods due to the removal of the material.

3. Results and discussion

3.1. Crack growth

Fig. 1 shows crack growth curves drawn in representation log v against K_I for B_2O_3 contents of $x = 0$ (Fig. 1a) and $x = 38$ mol% (Fig. 1b) in water and air, where v = crack growth velocity. The curves are the best fit concerning an exponential function (solid lines)

$$v = v_0 \exp\left(\frac{b}{RT} K_I\right) \quad (1)$$

and concerning a power law (dashed lines)

$$v = \frac{v_0}{K_{I0}^n} K_I^n \quad (2)$$

At the measurement in air the glass with 38 mol% B_2O_3 (Fig. 1b) has a significantly higher fracture toughness K_{Ic} and a more expanded region 2. The slopes in regions 1 and 3 are comparable for both glasses.

By measuring in water the glasses with small B_2O_3 contents are fitted by Equation 1 in a large interval

0022–2461/87 $03.00 + .12

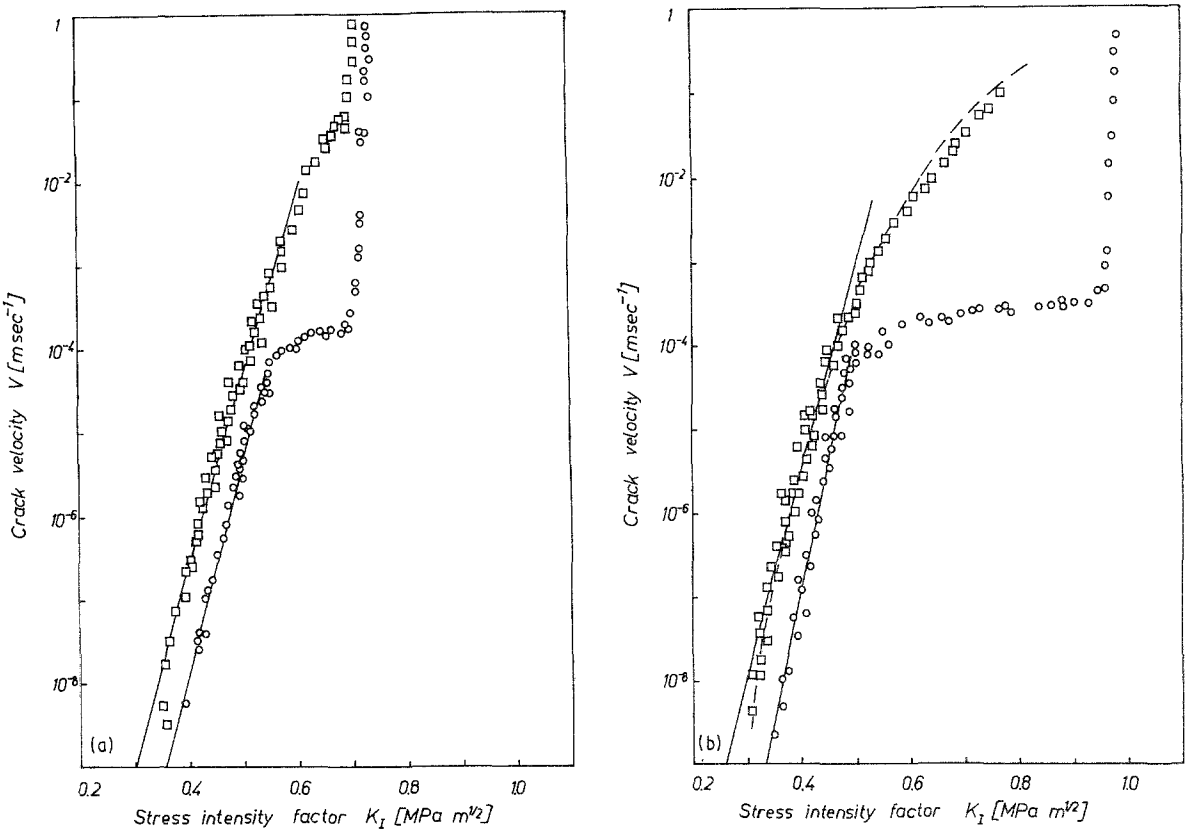

Figure 1 Crack growth curves of sodium alumosilicate glasses with different B_2O_3 content. □, Water; ○, air (50% r.h.). (a) $15Na_2O-4Al_2O_3-81SiO_2$, (b) $15Na_2O-4Al_2O_3-38B_2O_3-43SiO_2$.

of the crack growth velocity. Deviations appear for glasses with high B_2O_3 contents above 10^{-4} msec^{-1} and below 10^{-7} msec^{-1}. However, a better fit based on Equation 2 is possible in a larger interval. Furthermore, with increasing B_2O_3 content additional structures are generated on the smooth fracture surface at rates above 10^{-3} msec^{-1} (Fig. 2) due to an irregular corrosive attack of the water on the high loaded glass surfaces at the crack tip. The occurrence of the structures could be supported by material inhomogeneities and transport problems. In this crack growth region the fracture surface structures make it difficult or impossible to use the fracture surface modulation, whereas in region 3, which is not determined by corrosion processes, the fracture surfaces are smooth.

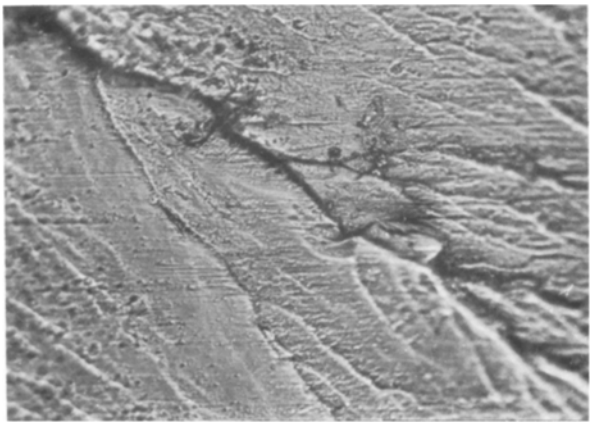

Figure 2 Fracture surface in the transition from region 1 to 2 in glasses with higher B_2O_3 contents.

3.2. Stress release rate, Young's modulus and inert strength

Fig. 3a demonstrates the influence of the B_2O_3 content on the fracture toughness K_{Ic} and the critical stress release rate G_c, respectively, as the energy based size. For a comparison the dependence of the Young's modulus, E, and the density, ϱ, is also shown in Fig. 3b. Both K_{Ic} and E increase up to a content of 20

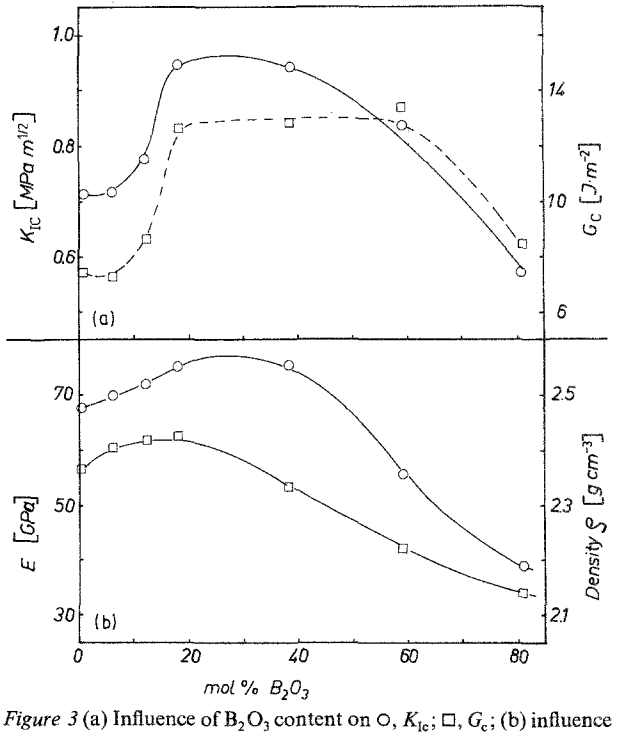

Figure 3 (a) Influence of B_2O_3 content on ○, K_{Ic}; □, G_c; (b) influence of B_2O_3 content on ○, E; □, ϱ.

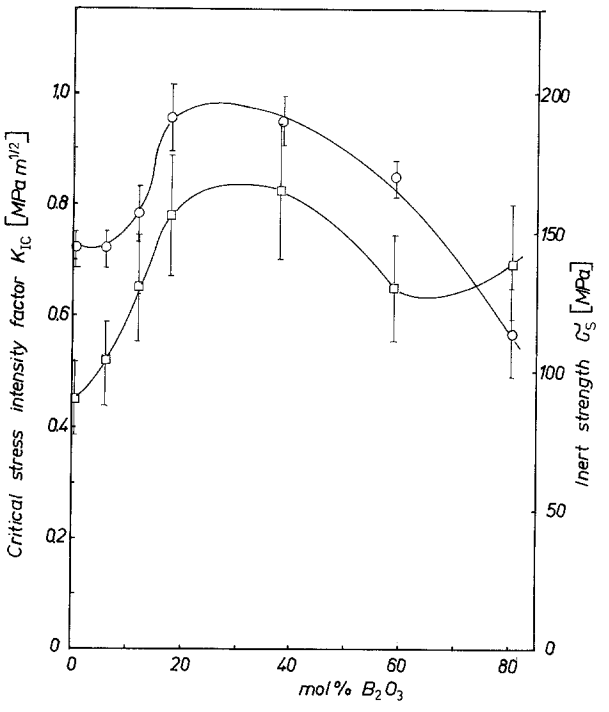

Figure 4 □, Inert strength σ_s and ○, fracture toughness K_{Ic} as functions of the B_2O_3 content of $15Na_2O$–$4Al_2O_3$–xB_2O_3–$(81\text{-}x)SiO_2$.

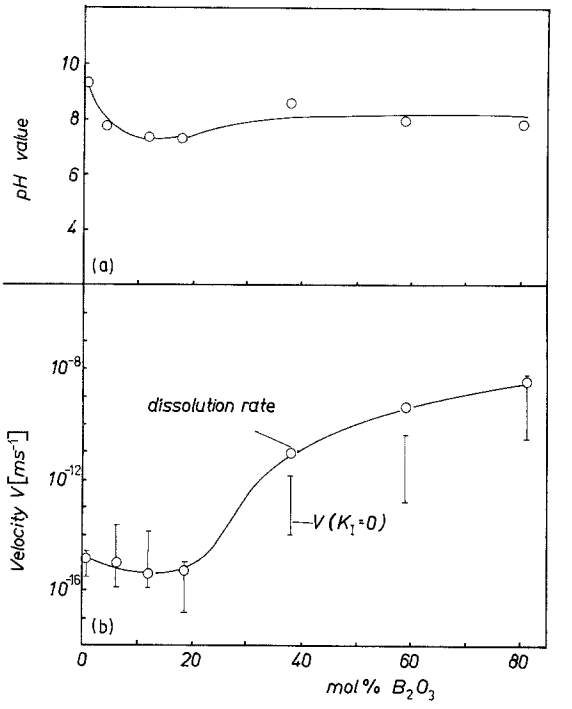

Figure 5 Influence of B_2O_3 content on (a) the pH value (ground glass–water slurry) and (b) the dissolution rate in comparison to the crack velocity v_0 at $K_I = 0$.

to 30 mol %, whereas above 40 mol % B_2O_3 a decrease is observed in analogy to Na_2O–B_2O_3–SiO_2 glasses [8].

The increase of the fracture toughness and the critical stress release rate, respectively, can be expected because the boron is arranged in four-fold coordination in this system up to 11 mol % and therefore the non-bridging oxygens are eliminated. The further increase of K_{Ic} above 11 mol % B_2O_3 content shows that the boron in three-fold coordination can also produce a strengthening of the network. Obviously the good mechanical properties are preserved as long as the [SiO_2]-tetrahedra form the dominating network. As Fig. 3b shows, a change of the mechanical properties for the worse is observed in correlation with a decrease of the density caused by an increasing build-up of a relatively separate borate network.

The question remains as to how the dependence of the inert strength reflects the above-mentioned circumstances. As Fig. 4 shows, the inert strength rises with increasing B_2O_3 content and reaches a maximum magnitude at 20 to 40 mol % B_2O_3 as K_{Ic}. However, the relative increase of the inert strength is higher than the one of the fracture toughness. In this connection we must consider that the inert strength depends not only on the fracture toughness but also on the glass-specific resistance against crack generation caused by a definite kind of mechanical damage. Therefore the higher relative increases of the strength can be attributed to a higher resistance of crack generation due to changed deformation behaviour at point loading on the surface. However, at high B_2O_3 contents, the observed return to the inert strength is based on reduced crack generation due to an occurrence of a leached surface layer.

3.3. Correlation to the dissolution rate

Let us now consider the influence of the B_2O_3 content on the dissolution rate in correlation with the crack growth velocity in region 1 in water (Fig. 5). The solid line shows the dependence of the dissolution rate of the plane glass surface (out of the cracks) on B_2O_3 content. The dissolution rate decreases slightly at small B_2O_3 contents ($10^{-16} < v < 10^{-15}$ msec^{-1}) and increases rapidly above 20 mol % up to values of $v \approx 10^{-9}$ msec^{-1} for the SiO_2-free glass. That means, the borate glass which is known to be very poorly resistant has a dissolution rate 10^7 times that of the more resistant borosilicate glass. It is of interest to note in which way the extremely different dissolution rates effect both the level and slope of the crack growth velocity in region 1.

The crack growth velocity v_0, determined by extrapolation to $K_I = 0$ according to Equation 1 is also shown in Fig. 5. Based on the stress corrosion theory, this velocity corresponds to the dissolution rate of glasses at the tip of the unloaded crack. The bars in Fig. 5 indicate the maximum variation of data. The dependence of v_0 on the B_2O_3 content is comparable with that of the dissolution rate, even if the two values differ at higher B_2O_3 contents.

The approximate correlation between dissolution rate and crack velocity at $K_I = 0$ in glasses with small B_2O_3 content supports the assumption that the crack growth is influenced by stress-accelerated network dissolution. Due to the slightly different slope n (Fig. 6) the level of the crack growth velocity in region 1 increases with the dissolution rate for every defined K_I value.

At higher B_2O_3 contents, corrosive modifications at the crack tip are possible (crack tip blunting, generation of leached layer) which can influence the slope and therefore the extrapolation to $K_I = 0$. Fig. 6 also shows that the slope b based on the exponential crack growth function, Equation 1, is influenced only slightly

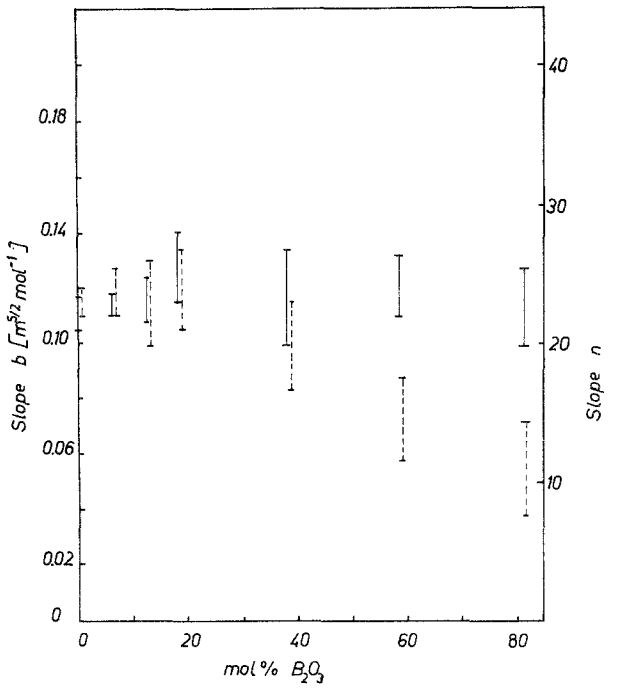

Figure 6 Dependence of the slopes (——), b and (– – – –), n in region 1 of the crack growth curves on the B_2O_3 content of $15Na_2O$–$4Al_2O_3$–xB_2O_3–$(81\text{-}x)SiO_2$.

by the dissolution rate. An indicated maximum is observed between 10 and 20 mol % B_2O_3.

This behaviour correlates to the pH value of ground glass–water slurry, which is a scale of the pH value at the crack-tip. In the upper portion of Fig. 5, the pH values are shown as a function of the B_2O_3 content. Except for the B_2O_3 free glass, the pH value varies within a small range ($7.3 < pH < 8.7$). Therefore the observed behaviour of the slope confirms the result of [3], according to which the slope of the crack growth velocity in region 1 is determined by the pH value at the crack tip.

The slope n based on the power law of crack growth, Equation 2, passes through a small maximum like slope b and decreases continuously at higher B_2O_3 contents. This is due to the usage of a larger range for the regression. The range includes also a part of the transition region toward the fatigue limit and the region a.

3.4. Dynamic fatigue and fatigue limit

A similar tendency of the slope can be observed by measuring the dynamic fatigue. Because of stronger surface corrosion of borosilicate glasses, in particular glasses with an increased B_2O_3 content, investigations of the fatigue behaviour have been of interest in order to study the effect of the leached layer generation and removal of material on the microcracks determining the strength.

In Fig. 7 the fracture strength σ normalized in all cases to the inert strength σ_s is plotted as a function of the stressing rate $\dot{\sigma}$ for some glasses of this system. With increasing B_2O_3 content at the beginning, the curves are shifted to lower strength values as a result of the increasing crack velocity and of broader region 2, respectively. Above 20 mol % the slope n decreases continuously from values of 20 to 23 to one of $n = 7$. These values are at the lower limit of the slope interval determined through crack growth measurements. On the one hand, the differences can be caused by the influence of the large transition region, while on the other hand, a water-containing layer of corrosion in the crack can be produced during the subcritical crack growth due to fast processes of the surface corrosion. These processes can influence the crack growth velocity [9, 10].

While at small B_2O_3 contents the fatigue curves can be calculated from crack growth data on the basis of a fracture-mechanical model with good precision, the correlation between macroscopic and microscopic crack growth is increasingly disturbed by corrosion processes. In practice, the fatigue limit is important. Starting from B_2O_3 free glass the relative fatigue limit is $\sigma_0/\sigma_S \simeq 0.37$ and it decreases with rising B_2O_3 content. At higher B_2O_3 contents a fatigue limit is observed at relative strength values $\sigma/\sigma_s \approx 0.2$. With increasing dissolution rate of the glasses the transition to the fatigue limit appears at higher stressing rates. The re-increase of strength at lower stressing rates is reinforced with increasing dissolution rate. This behaviour is interpreted by a corrosive change at the crack tip (crack tip blunting, alkali leaching) during the period until the load has risen to the start of crack growth.

In this context, the question arises as to which way

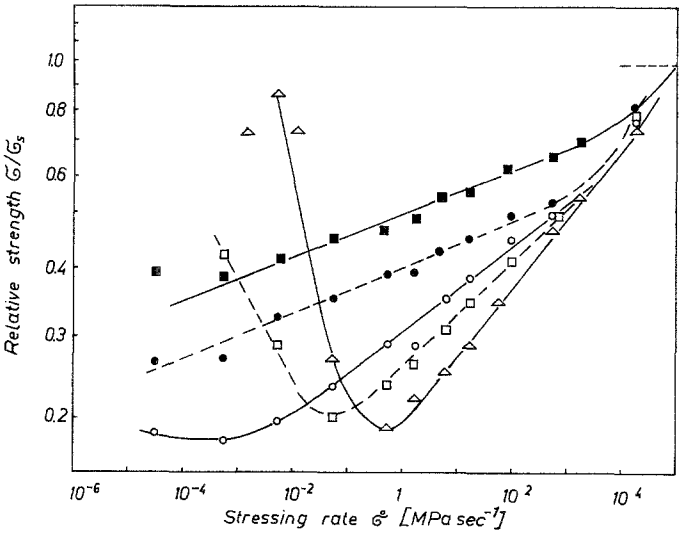

Figure 7 Normalized dynamic fatigue curves of glasses with different B_2O_3 content in water for $15Na_2O$–$4Al_2O_3$–xB_2O_3–$(81\text{-}x)SiO_2$. x = ■, 6; ●, 18; ○, 38; □, 59; △, 81.

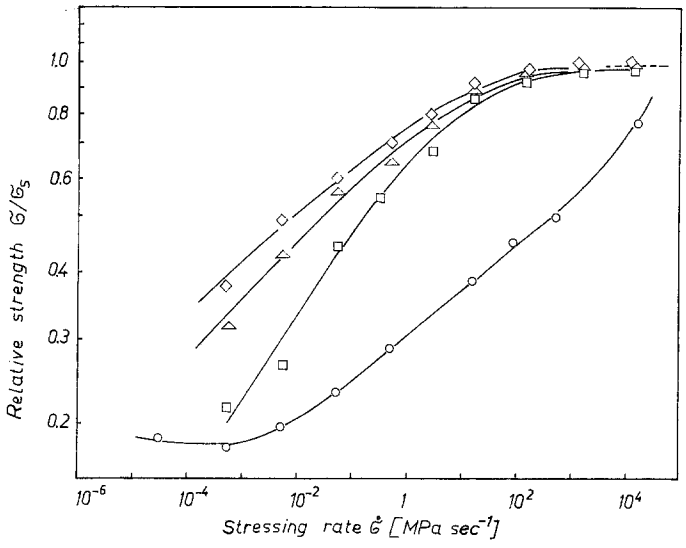

Figure 8 Influence of a corrosive pretreatment after the crack generation on the normalized fatigue curves of a glass with 38 mol% B_2O_3 ($15Na_2O$–$4Al_2O_3$–$38B_2O_3$–$43SiO_2$), after ageing in water for ◇, 24 h; △, 144 h; □, 456 h. ○, Immediately after abrasion.

the fatigue behaviour of the glasses is influenced by a corrosive pre-treatment after the crack generation. Fig. 8 shows the result of a selected glass aged in water for different time periods at room temperature. The values of the strength in Fig. 8 are normalized by the inert strength measured after ageing. The results demonstrate the complexity of the interaction between subcritical crack growth and surface corrosion in this glass system. While the rise of the inert strength and the shifting of the normalized fatigue curves toward smaller stressing rates indicate mechanisms retarding crack growth (such as crack tip blunting) the continuous decrease of the slope n could be caused by mechanisms accelerating crack growth. Corrosion layers with increased water content, involving a change of the mechanical properties at the crack tip, can stimulate the above mentioned mechanisms. The change of the slope n after ageing supports the previously made assumption that the differences between macroscopic and microscopic crack growth is caused by interfering corrosion processes.

4. Conclusions

1. Fracture toughness and Young's modulus show typical changes at the transition from silicate to borate glasses. A simple correlation to structural parameters does not seem to exist.

2. The correlation between crack growth and dissolution rate of the glasses supports the assumption that the crack growth is dominated by stress induced network dissolution within this system.

3. Dynamic fatigue and crack growth in the crack growth stimulated region show a nearly adequate behaviour. The transition to the fatigue limit is estimated by the dissolution rate in water.

References

1. S. M. WIEDERHORN and L. H. BOLZ, *J. Amer. Ceram. Soc.* **53** (1973) 543.
2. S. M. WIEDERHORN, *ibid.* **50** (1967) 407.
3. S. M. WIEDERHORN and H. JOHNSON, *ibid.* **56** (1973) 192.
4. C. J. SIMMONS and S. W. FREIMAN, *ibid.* **64** (1983) 683.
5. T. A. MICHALSKE and S. W. FREIMAN, *Nature* **295** (1982) 511.
6. H. RICHTER, *Glastechnische Berichte* **56K** (1983) 402.
7. E. GEHRKE, CH. ULLNER, M. HÄHNERT and G. BERGER, *Silikattechnik* **33** (1982) 238.
8. E. VERNAZ, F. LARCHE and J. ZARZYCKI, *J. Non-Cryst. Solids* **37** (1980) 359.
9. S. ITO and M. TOMOZAWA, *J. Physique* **43** (1982) 611.
10. E. GEHRKE and CH. ULLNER in Proceedings of the 9th ibausil-Conference, Weimar 1985, Vol. 4, p. 106–111.

Received 16 June
and accepted 18 August 1986